LA-UR-00-3109

Approved for public release;
distribution is unlimited

Title:

Optimum Design of Ultrahigh Strength Nanolayered Composites

Author(s): Harriet Kung*[,1], David Embury[2], Richard Hoagland[2], Amit Misra[1], Marc Verdier[1], John Hirth[2], Mike Nastasi[1], Terry Mitchell[1], Mike Hundley[3], Marilyn Hawley[1], Art Voter[4], and Sriram Swaninarayan[1]
[1] MST-8, [2] MST-DO, [3]MST-10, [4] T-12

Submitted to: DOE Office of Scientific and Technical Information (OSTI)

Los Alamos
NATIONAL LABORATORY

Form 836 (10/96)
ST 2629

Optimum Design of Ultraghigh Strength Nanolayered Composites

Harriet Kung*[,1], David Embury[2], Richard Hoagland[2], Amit Misra[1], Marc Verdier[1], John Hirth[2], Mike Nastasi[1], Terry Mitchell[1], Mike Hundley[3], Marilyn Hawley[1], Art Voter[4], and Sriram Swaninarayan[1]
[1] MST-8, [2] MST-DO, [3]MST-10, [4] T-12

Abstract

Refinement of the microstructures in metallic multilayers from the micrometer-scale to the nanometer-scale often results in a break down of classical Hall-Petch model relating strength to the microstructural length scale. The critical length scale at which this behavior breaks down is investigated both experimentally and theoretically. We evaluated the microstructure and mechanical properties of Cu/Cr, Cu/Ni, and Cu/Nb multilayers having different shear moduli mismatch between layers and lattice misfit strain between layers by transmission electron microscopy and nanoindentation. Two-dimensional maps showing layer thickness and grain size ranges over which different deformation mechanisms operate were constructed using dislocation theory. The deformation mechanisms responsible for the breakdown of Hall-Petch behavior are discussed. By correlating the deformation mechanism maps with the experimental data, we show that these maps serve as guidelines for interpreting the scale-dependent deformation mechanisms in multilayers. Atomistic simulation was also used to evaluate the interaction between interfaces and glide dislocations to provide atomic scale insights into the deformation mechanisms.

Background and Research Objectives

The physical dimensions of materials can, in some very important circumstances, exert a strong influence on intrinsic properties, particularly when the dimensions become very small. The reduction of structural scale to the nanometer range has been shown to be *a gateway to a realm of matter with unusual characteristics and a wide range of unique properties*. For example, solutions of semiconductor nanoparticles fluoresce in different colors, depending on the particle size; TiO_2 particles can change from hydrophobic to hydrophilic upon UV exposure when the particle size is below 20 nm; and the quantum confinement effect in quantum dots and nanowires may significantly change their electronic structure [R1-2].

Mathematical descriptions of matter often involve assumptions or approximations that may not, in some instances, be appropriate as the size scale approaches the nanometer range. For example, the descriptions which apply to 3D periodic, infinite media provide poor descriptions of electronic structure near surfaces and in films and nanowires. Similar

hkung@lanl.gov

problems exist in the mechanical properties of ultrafine-scale materials. In ultrafine-scale materials, confinement to regions with nanometer length-scales can significantly alter the role of dislocations in controlling strength and toughness relative to larger scale versions of the same material. Also, in such materials, interfaces may become the dominant microstructural feature.

In general, materials behavior changes dramatically when structural dimensions approach the nanometer range. The potential for capturing the extraordinary engineering capabilities that may be afforded by ultrafine-scale microstructures requires a substantial advancement of the current understanding of the relation between atomic scale structure and mechanical properties. The objectives of this LDRD program are to elucidate the relationship between macroscopic mechanical behavior and microscopic mechanisms involving the movement, storage, and recovery of dislocations in the crystalline phases and the interfaces between them. Through this understanding we seek to obtain general scaling laws that describe the transitions between mechanisms in terms of the modulation wavelength and interfacial structure. The major goals of this study are: 1) gaining atomic scale insight into strengthening mechanisms in nanoscale materials, and 2) developing a comprehensive theory that will relate changes in structure to changes in mechanical behavior.

Importance to LANL's Science and Technology Base and National R&D Needs

A fundamental understanding of the strengthening mechanisms in multilayers is urgently needed for advancing current knowledge regarding some very fundamental issues in nanophase materials. Scientific issues are: the limits to conventional deformation mechanisms such as Hall-Petch and Orowan descriptions of yielding as microstructural scale reduces to the nanometer scale; the new mechanisms governing deformation that may come into play at these very small dimensions, and the role of defects and bonding at interfaces. From a technological standpoint, establishing a fundamental understanding relating the microscale structure/strengthening mechanisms to macroscale properties is crucial to the development of nanolayer based materials as well as to the future revolution of the materials design.

The potential range of applications for ultrahigh-strength, ductile materials can be enormous. Achieving a reduction in size without loss of load-carrying integrity has many

hkung@lanl.gov

implications for areas such as architecture, power production and transmission, magnets, transportation, and robotics to name a few. The maturation of concepts that enable the design and fabrication of such materials could also have a revolutionary impact on understanding the integrity of various small-scale electronic devices. Similar advantages are obvious in the development of MEMS (micro-electro-mechanical-systems).

Scientific Approach and Accomplishments

Materials and Microstructures

Cu/Nb, Cu/Ni, and Cu/Cr multilayers and single layered Cu, Nb, Ni, and Cr films were deposited by either dc sputtering or e-beam evaporation on {100} Si single crystal substrates. The multilayers consist of alternating Cu and X (X is Cr, Ni, or Nb) layers of equal thickness, and the total thickness of the multilayered and single layered thin films was ~1 μm. Transmission electron microscopy (TEM) was performed on a Philips CM30 microscope, and high resolution TEM (HRTEM) was performed on a JEOL 3000F microscope, both microscopes were operated at 300 kV. The detailed procedures for film growth and TEM sample preparations have been reported previously [P2-7].

Both Cu/Nb and Cu/Cr are fcc/bcc systems and the individual layers are polycrystalline with columnar grains. The interfaces are parallel to $\{110\}_{bcc}$ and $\{111\}_{fcc}$, which are the close-packed planes of bcc and fcc metals, respectively. There is a strong texture between the Cu layers and the bcc metal (Nb or Cr), with $<110>\{111\}_{Cu}$ // $<111>\{110\}_{Nb\ or\ Cr}$, i.e. there is a Kurdjumov-Sachs orientation relation between the close-packed planes and directions of the fcc Cu and the bcc. Nb or Cr. The modulus mismatch between Cu and Nb is significantly lower than that between Cu and Cr. Further, the interface misfit for $\{110\}_{bcc}$ and $\{111\}_{fcc}$ planes is ~2.5% for Cu/Cr and ~10.5% for Cu/Nb [P11]. The microstructure of a Cu/Cr multilayer with layer thickness of 100 nm (i.e., bilayer period of 200 nm) is shown in Figure 1. This cross-section TEM micrograph shows the columnar microstructure in both layers. Using TEM micrographs from a range of layer thicknesses, we deduced the following relationships between layer thickness (h) and the in-plane grain size (d) in the Cu layers: $\ln(d) = 0.21 + 0.82 \ln(h)$ for Cu/Cr system, and $\ln(d) = 2.1 + 0.45 \ln(h)$ for Cu/Nb system, where d and h are in nm. A linear relationship between ln (h) and ln (d) in sputtered films has

hkung@lanl.gov

also been observed by other investigators, and is believed to be consistent with a normal grain growth process during deposition at room temperature [P27,R3-4].

In contrast, by first growing a single crystalline seed layer of Cu on {100} Si substrate at 400°C, Cu/Ni multilayers exhibit an epitaxial growth as shown in a HRTEM image of the Cu/Ni interface in Figure 2. A detailed account of the microstructure and mechanical behavior of the Cu/Ni multilayers has been reported in [P17,P26]. The lattice mismatch is accommodated by misfit dislocations, as indicated by a white dislocation symbol in Figure 2. The differences in the microstructure and physical properties of the three composite systems are compared and listed in Table 1.

hkung@lanl.gov

Table 1 A comparison of the composite systems investigated

System	Mutual Solubility	Interface Misfit *	G_X/G_{Cu}**	Orientation Relationship
Cu/Nb	immiscible	10.5 %	0.8	Kurdjumov-Sachs***
Cu/Cr	immiscible	2.3 %	2.4	Kurdjumov-Sachs***
Cu/Ni	completely miscible	2.5 %	1.5	cube-on-cube

* For fcc/bcc systems, % misfit between interplanar spacings of {110}bcc and {111}fcc; for fcc/fcc systems, % misfit between interplanar spacings of {100}Cu and {100}Ni.
** where G_{Cu} is shear modulus of Cu and G_X is shear modulus of the other phase

*** Orientation relation with $<110>\{111\}_{Cu}$ // $<111>\{110\}_{Nb \text{ or } Cr}$

Mechanical Properties

Mechanical properties were evaluated by nanoindentation using a Nano Indenter® II instrument. The nominal indentation depth was 150 nm. Other experimental details are presented elsewhere [P11-12,P17,P26]. The hardnesses of these composite films measured by nanoindentation are plotted as a function of $1/\sqrt{h}$ in Figure 3. For all three composites, hardness varies linearly with $1/\sqrt{h}$ for $h \geq 50$nm. A linear fit to the data in Figure 3 for $h > 50$ nm is consistent with the Hall-Petch (H-P) model, $\sigma = \sigma_o + k/\sqrt{h}$. The y-intercept from the linear fit corresponded to the hardness of the 1 μm Cu film for each of the three composites. At length scales below the breakdown of H-P hardening, the hardness increases only gradually with decreasing h up to ~10 nm. At even lower h, hardness may be independent of h (as in the Cu-Cr system) or softening may be observed (as in the Cu-Ni). However, in Cu-Nb system a gradual increase in hardness is observed as the layer thickness approaches 2.5 nm. Hence, as the microstructural scale is decreased from sub-micrometer to nanometer, four stages are observed in the scale dependence of strength (σ): (i) H-P dependence, $\sigma \propto h^{-1/2}$, (ii) modified H-P dependence $\sigma \propto h^{-a}$ where $a \neq 0.5$, (iii) σ is independent of h, and (iv) σ decreases with decreasing h. While stages (i) and (ii) are common to almost all the systems studied here and by other investigators [P23], the stages (iii) and (iv) are observed in some systems only in room temperature indentation tests. Note that since d scales with h, similar trends would be observed if H is plotted with $1/\sqrt{d}$.

In the H-P regime, Figure 3 shows that the slope is higher for Cu/Cr as compared to Cu/Nb and this has been attributed to the higher shear modulus mismatch in the former system

[P11]. The lower slope in the Cu-Ni system is presumably related to the epitaxial nature of these multilayers with a cube-on-cube orientation relationship that allows perfect matching of slip systems across the interface. A detailed discussion on the comparison of the three Cu-based systems was documented in [P11].

Theoretical Approach and Results

The experimental results shown in the previous section can be interpreted using dislocation theory. In particular, we seek to understand the breakdown of Hall-Petch type hardening below a critical microstructural scale in polycrystalline multilayers. Several attempts have been made to calculate the limits to the pile-up behavior as a function of a single microstructural length scale [R5-7]. Recently we have developed an approach to incorporate both grain size and layer thickness in the analysis of pile-up behavior in polycrystalline multilayers [P28]. For the type of microstructure shown in Figure1, we assume that the interface misfit (ε_{misfit}) is compensated by an array of edge dislocations with spacing λ. We further assume that initial yield in the softer phase (Cu in the present case), would lead to screw dislocation pile-ups at the grain boundaries in the Cu layer. By balancing the back stress of the screw dislocation pile-up with the back stress of the edge array, we obtain the following equation that relates the number of dislocations in the screw pile-up (n) to d, h and λ: $d = 8n\lambda/\{3\pi \coth(\pi h/2\lambda)\}$

For a given system (and hence, a given λ), the locus of d and h can be plotted for any given value of n. The above equation defines the limits of pile-up behavior for $d \approx h$ and $d < h$. For the case of $h << d$ (i.e., almost single crystal layers), we need only one dimension to define the transition length scales (h_t). For this case, we need only consider a pile-up at the interface and use the following equation [R8] that relates n, h and applied shear stress (τ): $n = (1-\upsilon)\, h\, \tau / Gb$, where G is the shear modulus, ν is Poisson ratio and b is the Burgers vector of the softer phase. A lower-bound on τ may be obtained using the coherency stress (σ_{misfit}) which can again be estimated knowing ε_{misfit}. Hence, knowing ε_{misfit}, b and υ, one can calculate h_t for a given n. Based on these elaborations, we can construct two-dimension plots of d vs. h that define length scales corresponding to $n > 2$ (continuum pile-up behavior), n=2 (discrete pile-up behavior), and n=1 (single dislocation behavior). Finally, we postulate that when the microstructural scale is so fine that the Orowan stress, Gb/h, approaches the theoretical strength, G/10, the deformation mechanism may not involve dislocation bowing and

alternative mechanisms may be involved. Thus, using only ε_{misfit}, b and υ for a given system, we can make predictions that correlate microstructural length scales with the maximum number of dislocations can be accommodated in the pile-up. The results of the theoretical calculations for ε_{misfit} =2.5%, (e.g. Cu/Cr or Cu/Ni system), are shown in Figure 4. The results of these calculations compared very well with the experimental results, and the comparison has been reported recently [P32].

Atomistic Simulations

Atomistic modeling was used to explore different mechanisms that control or play important roles in determining the strength of metallic composites in which the microstructurally important length scales is measured in nanometers. It is especially notable that conventional deformation mechanisms that are well understood in terms of their contribution to microscopic and macroscopic mechanical properties play a secondary role, or, in some cases, are irrelevant in nanoscale materials. We have been interested in deformation mechanisms important to nanoscale materials but that are either poorly understood or had been previously unknown. Interfaces are a very important microstructural feature in nanoscale, metallic composites. As part of the atomistic studies, we have examined the interaction between glide dislocations and interfaces in copper-nickel multilayer systems.

As compared with the Cu/Ag system, we find that an interface between Cu and Ni is much stronger, i.e., is more resistant to slip. Indeed, a coherent Cu/Ni interface (the copper and nickel layers are both strained such that the lattice parameters match at the interface) displays unusual behavior as shown in Figure 5. This figure shows the response of the system to a very large shear stress, about 2.5 GPa, in which a dissociated screw dislocation has moved through the copper to the interface and then cross-slipped back into the copper. Similar results were found with other types of dislocations. Consequently, this interface is opaque to slip, for reasons associated with the very high stresses caused by coherency.

Long range stresses typical of a coherent system are removed as the system is allowed to become semicoherent through the introduction of misfit dislocations on the interface. However, there remain significant short-range stresses, typical of a planar array of edge dislocations. Under these circumstances, we find the slip is able to more easily penetrate the interface and an example of this in the semicoherent Cu/Ni system is shown in Figure 6. The

applied stresses required to penetrate the semicoherent interface are about one third that at which cross-slip occurred in the coherent interface shown in Figure 5. Clearly, this semicoherent interface is now much more transparent to slip. Perhaps even more interesting, however, is that it is not uniformly transparent, as some portions of the interface, particularly near the misfit dislocations, are more resistant to slip transection than others. These results provide invaluable insights into the atomic-scale mechanisms involved in slip transfer in nanostructured materials.

Electrical Resistivity and Residual Stress Measurements

We have also investigated the parallel (in-plane) electrical resistivities of single-layered Cu and Cr films, and Cu/Cr multilayered thin films, as a function of layer thickness. The resistivities were measured in the temperature range of 4-325K. The resistivity of the multilayers at a given temperature increased, and the residual resistivity ratio decreased with decreasing layer thickness. At 300K, the resistivity of a 1μm thick Cu film was approximately equal to bulk value, but the resistivity of the Cr film was an order of magnitude higher than that of bulk Cr. The discrepancy is believed to be related to the columnar microstructure and very high residual stress in the Cr film. The dependence of electrical resistivity on the layer thickness of multilayers is explained using a model that accounts for interface scattering and thin-film resistivities of polycrystalline Cu and Cr. A detailed report of the work on electrical resistivity of Cu-based single phase and multilayered films has been published in [P19].

The evolution of intrinsic residual stresses in sputtered Cr thin films with substrate bias and post-deposition ion irradiation is also investigated. The relaxation of tensile stresses and build up of compressive stresses with increasing ion irradiation dose is studied using ions of different masses and energies. The stress evolution is related to the corresponding microstructural changes in the films. The changes in the residual stress during ion irradiation are explained by considering the manner in which the interatomic distances and forces change during irradiation, and the generation of defects during irradiation. A detailed account of the work has been published in [P14,P18,P20-21,P31].

Publications

P1. P.G. Sanders, M.N. Rittner, J.R. Weertman, and H. Kung, "Creep of Nanocrystalline Cu, Pd, and Al-Zr", Nanostructured Materials, **9**, 433 (1997).

P2. S. Fayeulle, M. Nastasi, Y-C. Lu, H. Kung, and J.R. Tesmer, "Thermal and Ion Irradiation Stability of DC Sputtered TiN-B-C-N", Applied Physics Letters, **70**, 1098 (1997).

P3. S. Fayeulle, M. Nastasi, Y-C. Lu, H. Kung, and J.R. Tesmer, "Ion Beam Induced Modifications in DC sputtered TiN/B-C-N Multilayers", Nuclear Instruments and Methods B, **127**, 198 (1997).

P4. Y.-C. Lu, H. Kung, T. R. Jervis, J.-P. Hirvonen, D. Ruck, T. E. Mitchell and M. Nastasi, "Effect of 690 keV Xe ion irradiation on the microstructure of amorphous $MoSi_2$/SiC nanolayer composites", Nuclear Instruments and Methods B, **127**, 648 (1997).

P5. T.E. Mitchell, Y.-C. Lu, A. J. Griffin Jr., M. Nastasi, and H. Kung, "Structure and Mechanical Properties of Cu/Nb Multilayers", Journal of Am. Ceram. Soc., **80**, 1673 (1997).

P6. Y.-C. Lu, H. Kung, A. J. Griffin, M. A. Nastasi and T. E. Mitchell, "Observations of dislocations in Cu/Nb nanolayer composites after deformation", J. Mater. Res., **12**, 1939 (1997).

P7. H. Kung, Y-C. Lu, A.J. Griffin, Jr., M. Nastasi, T.E. Mitchell, and J.D. Embury, "Observation of bcc Cu in Cu/Nb Nanolayered Composites", Applied Physics Letters, **71**, 2103 (1997).

P8. P.P. Freitas , M.C. Caldeira, M. Reissner, B.G. Almeida, J.B. Sousa, and H. Kung, "Design, fabrication, and wafer level testing of (NiFe/Cu)(XN) dual stripe GMR sensors", IEEE Transactions on Magnetics, **33**, 2905 (1997).

P9. H. Kung, Y.-C. Lu, A. H. Bartlett, R.G. Castro, J.J. Petrovic, and E. Shtessel, "Structural Characterization of Combustion Synthesized $MoSi_2$-Si_3N_4 Composite Powders and Plasma Sprayed $MoSi_2$-Si_3N_4 Composites", J. Mater. Res., **13**, 1522 (1998).

P10. J.D. Bryant, H. Kung and A. Misra "The Effects of Preaging Treatments on Precipitation in Al-Mg-Si Automotive Body Sheet Alloys", *Automotive Alloys II*, S.K. Das et al., eds., TMS, 1 (1998).

P11. A. Misra, M. Verdier, Y.C. Lu, H. Kung, T.E. Mitchell, M. Nastasi and J.D. Embury, "Structure and Mechanical Properties of Cu-X (X=Nb, Cr and Ni) Nanolayered Composites", Scripta Mat., **39**, 555 (1998).

P12. A. Misra, H. Kung, T.E. Mitchell, T. Jervis and M. Nastasi, "Microstructures and Mechanical Properties of Sputtered Cu/Cr Multilayered Thin Films", MRS Sym. Proc., **505**, 583 (1998).

P13. J-P. Hirvonen, P. Torri, R. Lappalainen, J. Likonen, H. Kung, T.R. Jervis, and M. Nastasi, "Oxidation of $MoSi_2$/SiC nanolayered composite", J. Mater. Res., **13**, 965 (1998).

P14. A. Misra, S. Fayeulle, H. Kung, T.E. Mitchell and M. Nastasi, "Effects of Ion Irradiation on the Residual Stresses in Cr Thin Films", Applied Physics Letters, **73**, 891 (1998).

P15. V. J. Keast, H. Kung, T. E. Mitchell and A. Misra, "Elemental Mapping of Nanoscale Cu/Nb Multilayers", in Electron Microscopy 1998, H. A. Calderón Benavides and M. José Yacaman, eds., Institute of Physics, Bristol, Vol. **III**, 563 (1998).

P16. D.S. Stone, M.F. Tambwe, H. Kung, and M. Nastasi, "Hardness of Thin Films Determined Based on Load and Contact Stiffness", MRS Sym. **522**, 257 (1998).

P17. M. Verdier, M. Niewczas, J.D. Embury, M. Hawley, M. Nastasi, and H. Kung, "Plastic Behaviour of Cu/Ni Multilayers", MRS Proc., **522**, 77 (1998).

P18. M. Nastasi, S. Fayeulle, Y.C. Lu , H. Kung, "The Influence of Stress During Ion-Beam Mixing", Mater. Sci. Eng., **253**, 202 (1998).

P19. A. Misra, M.F. Hundley, D. Hristova, H. Kung, T.E. Mitchell, M. Nastasi and J.D. Embury, "Electrical Resistivity of Sputtered Cu/Cr Multilayered Thin Films", Journal of Applied Physics, **85**, 302 (1999).

P20. A. Misra, S. Fayeulle, H. Kung, T.E. Mitchell and M. Nastasi, "Residual Stresses and Ion Implantation Effects in Cr Thin Films", Nucl. Inst. and Methods B, **148**, 211 (1999).

P21. S. Fayeulle, A. Misra, H. Kung and M. Nastasi**,** "Thermal annealing, irradiation, and stress in multilayers", Nucl. Inst. And Methods B, **148**, 227 (1999).

P22. H. Kung and T. Foecke, "Mechanical Behavior of Nanostructured Materials", MRS Bulletin, vol. **24**, No. 2, p.14, Feb. (1999).

P23. B.M. Clemens, H. Kung and S.A. Barnett, "Structure and Strength of Multilayers", MRS Bulletin, vol. **24**, No. 2, p. 20, Feb. (1999).

P24. J.R. Weertman, D. Farkas, K. Hemker, H. Kung, M. Mayo, R. Mitra, and H. Van Swygenhoven, "Structure and Mechanical Behavior of Bulk Nanocrystalline Materials", MRS Bulletin, vol. **24**, No. 2, p. 44, Feb. (1999).

P25. A.M. Baker, P.S. Grant, R.G. Castro, H. Kung, "Preliminary Characterization of a Plasma Sprayed MoSi2/Sigma SiC Fiber Monotape", Mat. Sci. and Eng. A -Structural

Materials Properties Microstructure and Processing, **261**, 196, (1999).

P26. M. Verdier, M. Hawley, J.D. Embury, and H. Kung, "Some Aspects of Plastic Deformation and Fracture in Cu/Ni Multilayers", *Constitutive and Damage Modeling of Inelastic Deformation and Phase Transformation*", ed: A.S. Khan, Neat Press, Maryland, 609 (1999).

P27. M.F. Tambwe, D.S. Stone, A.J. Griffin, H. Kung, Y. Cheng Lu, and M.Nastasi, "Haasen Plot Analysis of the Hall-Petch Effect in Cu-Nb Nanolayer Composites", J. Mater. Res., **14**, 407 (1999).

P28. A. Misra, M. Verdier, H. Kung, J.D. Embury, and J.P. Hirth, "Deformation Mechanism Maps for Polycrystalline Metallic Multilayers", Scripta Mat., **41**, 973 (1999).

P29. H. Kung, P.S. Sanders, and J.R. Weertman, "Transmission Electron Microscopy Characterization of Nanostructured Copper", *Advanced Materials for the 21st Century*, Edited by Y-W. Chung, D.C. Dunand, P.K. Liaw, and G.B. Olson, 455 (1999).

P30. P. Torri, J.P. Hirvonen, H. Kung, Y.C. Lu, M. Nastasi, P.N. Gibson, "Mechanical properties, stress evolution and high-temperature", J. Vac. Sci. Tech. B, **17**, 1329 (1999).

P31. A. Misra, H. Kung, T.E. Mitchell, and M. Nastasi, "Residual Stresses in polycrystalline Cu/Cr Multilayered Thin Films", J. Mater. Res. (2000), in press.

P32. A. Misra, M. Verdier, H. Kung, M. Nastasi, J.D. Embury, and J.P. Hirth, "Strengthening Mechanisms in Ultrafine-Scale Metallic Multilayers", submitted to "Ultrafine Grained Materials" edited by R.S. Mishra et al, Proceeding of TMS Annual Meeting 2000.

P33. M. Verdier, F. Spaepen, H. Huang, J.D. Embury, M. Hawley, H. Kung, "Effect of Scale on the Plastic Deformation of Cu/Ag Multilayers", submitted to Met Tran A (2000).

P34. K. Han, K. Yu-Zhang, H. Kung, J.D. Embury, B.J. Daniels, and B.M. Clemens, "f.c.c. to b.c.c. Transition in Fe/Pt Multilayers", submitted to J. Appl. Phys. (2000).

P35. H. Kung, Y-C. Lu, M. A. Nastasi, C. T. Necker, M. G. Hollander, P. D. Peralta and T.E. Mitchell, "Deposition of Cu/Ni multilayers on Cu single crystals by e-beam evaporation", submitted to JVST (2000).

References

R1. R. Wang, K. Hashimoto, A. Fujishima, M. Chikuni, E. Kojima, A. Kitamura, M. Shimohigoshi, and T. Watanabe, "Light-induced Amphiphilic Surfaces", Nature, **388**, 431 (1997).

R2. Z.B. Zhang, J.Y. Ying, and M.S. Dresselhaus, "Bismuth quantum-wire arrays fabricated by a vacuum melting and pressure injection process", Journal of Materials Research, **13**, 1745 (1998).

R3. D.B.S. Knorr and D.P. Tracy, "A review of microstructure in vapor-deposited copper thin-films", Mat. Chem. Phys., **41**, 206 (1995).

R4. C.R.M. Grovenor, H.T.G. Hentzell, D.A.Smith, "The development of grain-structure during growth of metallic-films", Acta Metall., **32**, p 773 (1984).

R5. R.W. Armstrong, Y.T. Chou, R.M. Fisher, and N. Louat, "The Limiting Grain Size Dependence of the Strength of a Polycrystalline Aggregate", Phil. Mag., **14**, 943 (1966).

R6. P.M. Anderson and C. Li, "Hall-Petch relations for multilayered materials", NanoStructured Materials, **5**, 349 (1995).

R7. T.G. Nieh and J. Wadsworth, "Hall-Petch relation in nanocrystalline solids", Scripta Metall. Mat., **25**, 955 (1991).

R8 J.P. Hirth and J. Lothe, *Theory of Dislocations*, Wiley, p 770 (1982).

Figure Captions

Figure 1: Cross-section dark field TEM micrograph showing the polycrystalline microstructure of Cu/Cr multilayers (h=100nm, d_{Cu} = ~50nm in this sample). Note that $d_{Cr} << d_{Cu}$.

Figure 2: HRTEM image showing the epitaxial relationship of Cu and Ni layers. The interface plane is close {100} of both Cu and Ni, and the misfit dislocation was indicated by a white dislocation symbol.

Figure 3: Hardness of Cu-Nb, Cu-Cr and Cu-Ni multilayers plotted as a function of $1/\sqrt{h}$ where h is one-half of the bilayer period.

Figure 4: Deformation mechanism map for multilayer systems with lattice misfit of 2.5% (e.g. Cu/Cr or Cu/Ni).

Figure 5: An atomistic model of a nickel (bottom layer) – copper (top layer) bilayer composite showing the trajectory followed by a screw dislocation in the copper in response to a shear stress applied parallel to the interface.

Figure 6: The same model shown in Figure 5, except that it contains two misfit dislocations (T symbols) located on the interface at the edges of the array. The dashed arrow indicates the trajectory of a mixed dislocation which has moved from the copper through the interface into the nickel in response to a tensile stress applied parallel to the interfacial plane.

hkung@lanl.gov

Figure 1

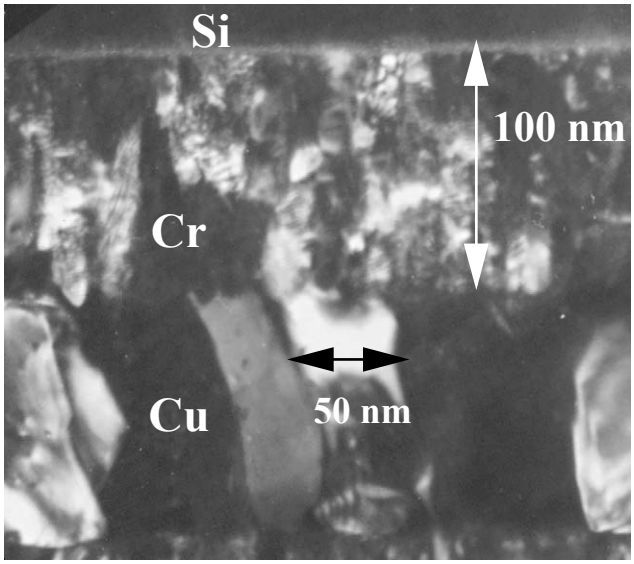

hkung@lanl.gov

Figure 2

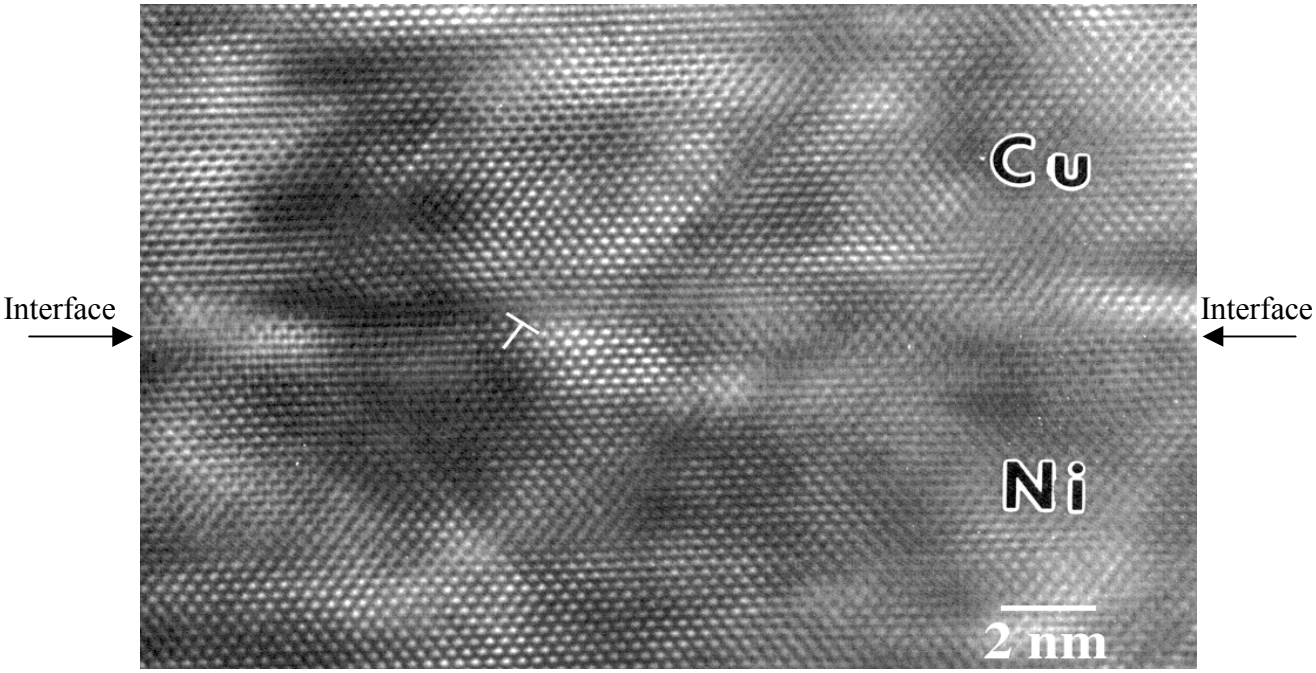

hkung@lanl.gov

Figure 3

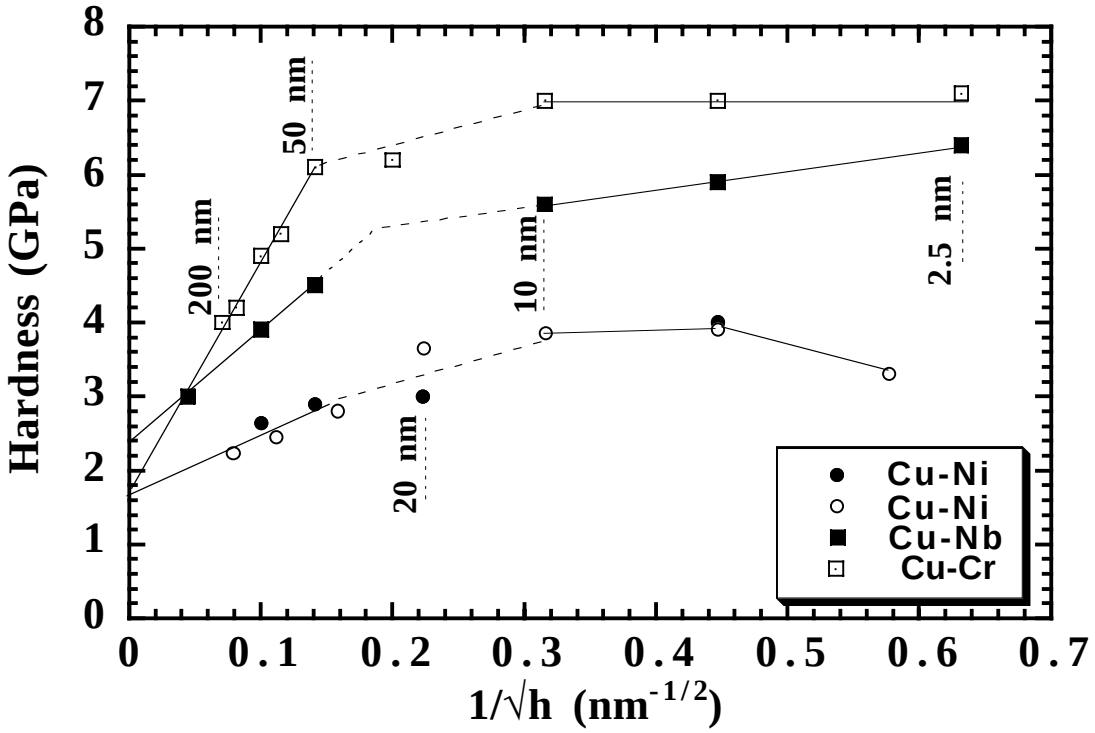
Hardness (GPa)
1/√h (nm^-1/2)
0
1
2
3
4
5
6
7
8
0
0.1
0.2
0.3
0.4
0.5
0.6
0.7
200 nm
50 nm
10 nm
2.5 nm
20 nm
Cu-Ni
Cu-Ni
Cu-Nb
Cu-Cr

Figure 4

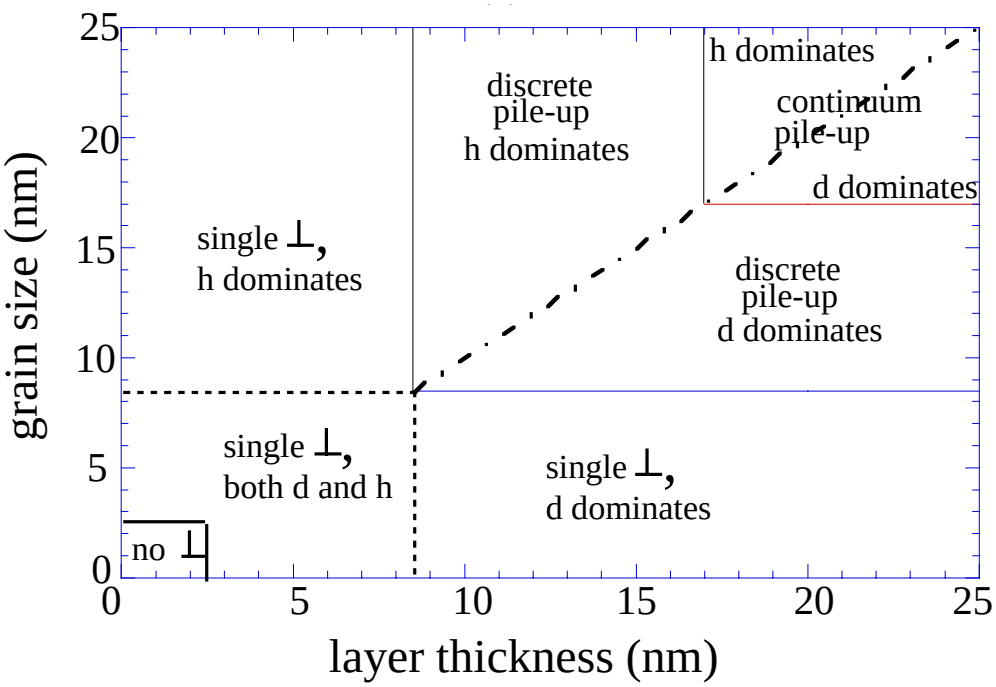
grain size (nm)
layer thickness (nm)
0
5
10
15
20
25
h dominates
discrete
pile-up
h dominates
continuum
pile-up
d dominates
single ⊥,
h dominates
discrete
pile-up
d dominates
single ⊥,
both d and h
single ⊥,
d dominates
no ⊥

Figure 5

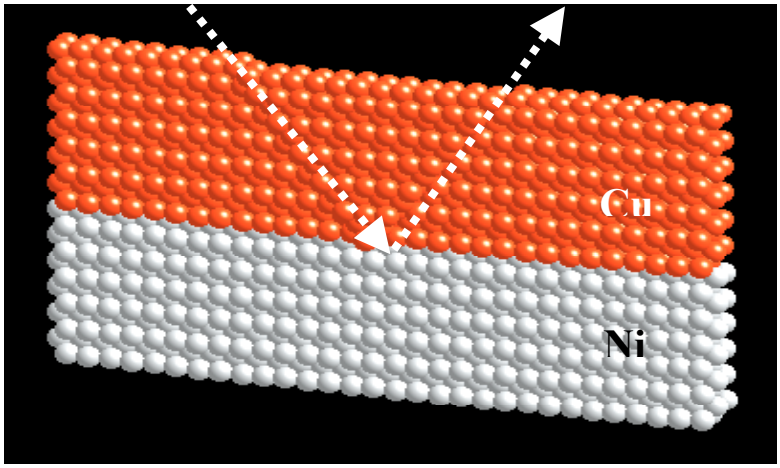

hkung@lanl.gov

Figure 6

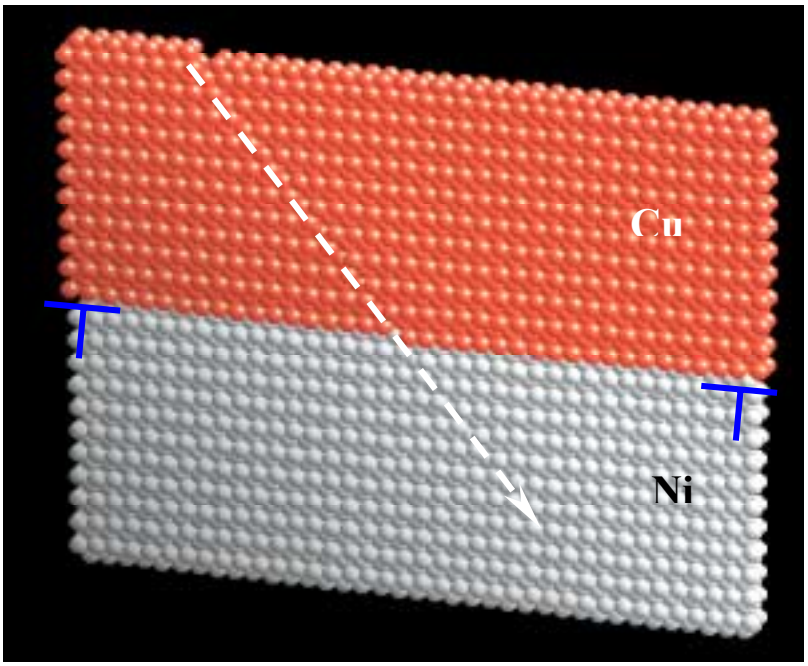

hkung@lanl.gov